

- 1 **Title:** *fasterRaster*: GIS in *R* using *GRASS* for large vectors and rasters
- 2 **Running title:** *fasterRaster*: GIS in *R* for large rasters
- 3 **Published in:** *Transactions in GIS*, doi: [10.1111/tgis.70238](https://doi.org/10.1111/tgis.70238)
- 4 **Author:** Adam B. Smith
- 5 **Affiliation:** Missouri Botanical Garden, 4344 Shaw Boulevard, Saint Louis, Missouri 63110
- 6 USA.
- 7 **Email:** adam.smith@mobot.org
- 8 **ORCID:** 0000-0002-6420-1659
- 9 **Conflict of Interest Statement:** I declare no conflicts of interest.
- 10 **Acknowledgements:** I thank Jeanne J. Smith for accompanying me in developing this software.

11 *fasterRaster*: GIS in R using GRASS for large rasters and vectors

12 **Abstract [150 words of 150]**

13 Within the R ecosystem, packages like *terra* and *sf* are the go-to solutions for most geospatial
14 analyses, yet can struggle with large rasters and vectors. The *Geographic Resources Analysis*
15 *Support System*, or *GRASS*, offers solutions that are often more efficient for large data. However,
16 using *GRASS* through R requires users to become familiar with *GRASS*-specific syntax and data
17 constructs. The *fasterRaster* package for R seamlessly connects to *GRASS* and enables analysis
18 of large data sets. Modeled after the functions in *terra*, *fasterRaster* possesses over 200 methods
19 for processing rasters and spatial vectors. *fasterRaster* also contains a growing number of
20 specialty functions for hydrological, remote sensing, and topographical analysis. For small
21 spatial objects, *terra* and *sf* will nearly always be faster, but for larger objects, *fasterRaster* can
22 be several times faster, and for very large objects, can succeed where other solutions fail. A
23 *pkgdown* website contains documentation and a tutorial:
24 <https://adamlilith.github.io/fasterRaster/index.html>.

25 **Keywords:** geographic information system; geomorphology; hydrology; open source; geospatial;
26 scalability; memory management

27 **Main text [3938 words including main text, acknowledgements, figure captions, and table]**

28 **Introduction**

29 The growth in information-dense geographic data sets has enabled the asking and answering of
30 key questions in the environmental sciences, while at the same time demanding increasing
31 compute power. Rasters with very fine resolution and broad extents, and spatial vectors with
32 many features and fine-scale detail can take substantial time to process. Thus, there is a need for
33 tools that can process large rasters and vectors in an efficient manner.

34 The R ecosystem provides a flexible set of tools for analysis of geographic data. These include
35 the *sf* package for vectors (Pebesma, 2018; Pebesma & Bivand, 2023), and *terra* and *stars*
36 packages for both rasters and vectors (Hijmans, 2025; Pebesma & Bivand, 2023). Of note, the
37 *terra* package achieves significant gains in speed and memory management by processing
38 through compiled C++ code and, where possible, by leaving large rasters and vectors on disk to
39 be called in chunks as needed (Hijmans, 2025). Together, *terra*, *sf*, and *stars* provide the basis
40 for many dependent packages, and so form the mainstay for nearly all analyses of geographic
41 data within R. Nonetheless, large rasters and vectors can surpass the capacity of these tools, and
42 otherwise take substantial time to process when they do work.

43 *Geographic Resources Analysis Support System (GRASS)* is a powerful, open-source geographic
44 information system that handles raster and vector data (Neteler et al., 2012; *GRASS* Development
45 Team 2025a and b). *GRASS* supports many standard and specialty GIS operations through

46 “tools” (functions). These can be called via a command line, or through the built-in graphical
47 user interface.

48 Users familiar with *terra*, *sf*, and *stars* face barriers to harnessing the performance gains of
49 *GRASS*. Within *R*, users can call *GRASS* tools through the *rgrass* package (Bivand et al., 2025).
50 However, this requires users to become familiar with *GRASS* syntax, file organization, and data
51 “templates”. To start, users would first need to create a *GRASS* “project,” which is a working
52 folder in which support files and rasters and vectors with the same coordinate reference system
53 are stored. If GIS objects with a different coordinate reference system are used, a new project
54 needs to be created, and *GRASS* needs to be prompted to switch to the new project. Each project
55 also contains one or more “mapsets,” which are subfolders in which rasters and vectors are
56 stored. Mapsets must thus also be managed. Finally, each project has a “region,” which is a
57 dynamic, gridded object like a raster that has an extent and resolution. Most *GRASS* tools that
58 operate on rasters will automatically crop and resample the output to the extent and resolution of
59 the active region. Users must therefore track the region and modify it to ensure outputs have the
60 expected properties. Users of *terra*, *sf*, and *stars* do not have to manage analogous file
61 organization systems and data templates. Together, these differences create barriers to combining
62 the respective strengths of *terra*, *sf*, and *stars* with *GRASS*.

63 Here I present the *fasterRaster* package for *R*, which allows users of *R* to take advantage of the
64 capabilities of *GRASS*. *fasterRaster* uses *rgrass* as a backend to connect to *GRASS* (Bivand et al.,
65 2025), and so obviates the need to learn *GRASS*-specific syntax and file organization.
66 Importantly, *fasterRaster* is a complement, not a replacement, to *terra*, *sf*, and *stars*. Indeed,
67 *terra* and *sf* will often be more efficient for processing small- or medium-sized spatial objects.
68 However, for large rasters and vectors, *fasterRaster* can achieve significant performance gains
69 and enable analyses that are not otherwise possible using these tools.

70 *Software design*

71 *fasterRaster* was developed with five design principles in mind:

72 *Value-added*: *fasterRaster* was written to add value to existing tools, not to supplant
73 them. The *rgrass* package already provides a convenient bridge between *R* and *GRASS*, and
74 *fasterRaster* further facilitates this connection.

75 *Interoperability*: The large majority of *fasterRaster* methods (functions) share the same
76 name and functionality as methods in *terra*, and most share the same arguments. *fasterRaster*
77 uses *R*’s object-oriented programming system so users can use *terra*, *sf*, *stars*, and *fasterRaster* in
78 the same *R* session without conflict between methods that have the same name.

79 *Comparability*: *fasterRaster* functions are designed to yield output as similar as possible
80 to methods of same name in *terra*. For example, the *terra* function `focal()`, run with the `fun`
81 `= 'sd'` argument, calculates the sample standard deviation across a moving window of cells.
82 The equivalent tool in *GRASS*, `r.neighbors`, calculates the population standard deviation.

83 However, the *fasterRaster* version of `focal()`, by default, has been engineered to calculate the
84 sample standard deviation, though it also offers the option to calculate the population standard
85 deviation.

86 *Simplicity: fasterRaster* makes using *GRASS* in *R* simple. Users do not need to manage or
87 even be aware of *GRASS*-specific data constructs like projects, mapsets, or regions. These are
88 managed dynamically and automatically in the background.

89 *Ease-of-use: fasterRaster* makes *GRASS* tools easy to use. Functions have *R* help pages,
90 each with worked examples. The package has its own *pkgdown* website (Wickham et al., 2025)
91 with documentation and vignettes, including a “getting started” tutorial
92 (<https://adamlilith.github.io/fasterRaster/index.html>).

93 *Functionality*

94 *fasterRaster* can be installed from the Comprehensive R Archive Network (CRAN), with
95 development versions available from the GitHub repository at
96 <https://github.com/adamlilith/fasterRaster>.

97 After attaching the package using `library(fasterRaster)`, users must tell *fasterRaster*
98 where *GRASS* is installed on their system using the `faster()` function. (Help for this function
99 and any other can be obtained using `?functionName`.) After this, the first function call that uses
100 *GRASS* as a backend will start *GRASS*. Invisible to the user, *fasterRaster* creates a *GRASS*
101 “project” which is by default in the operating system’s temporary directory. *GRASS* will store
102 here all files it needs to do processing.

103 *fasterRaster* rasters and vectors are S4 objects called “GRasters” and “GVectors” (collectively,
104 “G-objects”). GRasters can contain integers, double-floating point numeric values, or categorical
105 data such as land cover classes. GVectors can have data tables, where each row corresponds to a
106 particular “geometry” (point, line, or polygon) in the vector. The `fast()` function can be used to
107 directly load from disk rasters or vectors in common file formats (e.g., GeoTIFF, Esri shapefiles,
108 or Open Geospatial Consortium GeoPackages). `fast()` can also convert rasters and vectors
109 from *terra* or *sf* packages to G-objects, although loading files from disk will always be faster
110 than coercing them from objects created by other packages. GRasters and GVectors are *R* objects
111 that contain pointers to *GRASS* files in the temporary *GRASS* project folder. Once the *R* session
112 is stopped, this temporary directory is typically emptied and the files within them will no longer
113 be available. To use G-objects in later analyses, users must save them using `writeRaster()` or
114 `writeVector()`, both of which can write files in a variety common file formats.

115 Users can apply any of >200 methods, including functions for cropping, buffering, masking,
116 projecting between coordinate reference systems, and otherwise creating and manipulating G-
117 objects. All of these methods can be perused through the package index using `?fasterRaster`
118 or on the *pkgdown* website. Of note, the package includes methods that draw on *GRASS*’s deep
119 array of specialty tools. For example, `geomorphons()` identifies topographic features from an

120 elevation raster (e.g., flat areas, pits, valleys, footslopes, spurs, peaks, etc.; Stepinski &
121 Jasiewicz, 2011; Jasiewicz & Stepinski, 2013). The `flow()`, `flowPath()`, and `streams()`
122 functions conduct hydrological analysis of watershed basins and stream flow. An array of
123 functions create rasters *de novo* with, for example, fractal geometry, random walks, normally
124 distributed values, or spatial dependence (`fractalRast()`, `rWalkRast()`, `rNormRast()`,
125 and `rSpatialDepRast()`, respectively). The `vegIndex()` function calculates 17 different
126 vegetation indexes including the normalized difference vegetation index (NDVI), enhanced
127 vegetation index (EVI and EVI2), normalized difference water index (NDWI; Gao 1996), and
128 the modified soil adjusted vegetation index (MSAVI; Qi et al. 1994). `bioclims()` generates the
129 19 BIOCLIM variables representing climatic extremes and averages (Booth et al., 2014) plus an
130 extended set of 20 additional BIOCLIM variables such as temperature or precipitation of the
131 quarters following the warmest/coldest quarters (i.e., fall or spring) and the
132 hottest/coldest/wettest/driest months or quarters. The `fragmentation()` function classifies
133 degrees of habitat fragmentation (i.e., patch, perforated, transitional, edge, interior; Riitters et al.
134 2000).

135 Workflows focused on “small” rasters and vectors (i.e., small number of cells and/or number of
136 vector features) will almost always run faster using *terra* functions, but *fasterRaster* can make
137 workflows faster—or at least feasible—if objects are large. To illustrate the strengths of each
138 package, I constructed two matching workflows for assessing the relative influence of drivers
139 and risks of forest loss in Southeast Asia. One workflow used almost exclusively *terra* methods,
140 and the other *fasterRaster* methods, but both were otherwise the same in the inputs, function
141 calls, order of operations, and outputs. Since actual performance will vary across different users’
142 workflows and data, the exercise is intended to be illustrative. Nonetheless, the comparison
143 demonstrates the relative tradeoffs between *terra* and *fasterRaster* and how to use each to best
144 advantage.

145 **Methods**

146 The study region encompassed five major river basins of Southeast Asia, the Mekong, Salween,
147 Irrawaddy, Chao Phraya, and the Sittang. In the past few decades, these regions have
148 experienced dramatic social and environmental change yet remain bastions of biodiversity
149 (Hughes 2017; Wang et al. 2023). Within the focal region, I used rasterized forest presence at
150 ~30-m resolution in 2000 and 2020 from Hansen et al. (2013). From these rasters, two states
151 (persistent versus lost) were scored (forest gain was negligible, so was ignored). A variety of
152 predictors demonstrated to influence forest loss and persistence were collated, including distance
153 to roads and rivers, elevation, slope, human population density, presence of agriculture, country,
154 protected areas status, and forest fragmentation class (Table S1). Generalized linear models were
155 constructed across 50 cross-validation folds, and the resulting prediction rasters averaged to
156 create a map of the risk of forest loss.

157 The two workflows relied either primarily on *terra* or *fasterRaster*, with minimal use of the
158 opposing package in each package’s workflow. The workflows employed a variety of common
159 geographic operations. For rasters, these included projecting, resampling, merging, cropping,
160 masking, and mathematical operations on rasters, plus focal (neighborhood) analyses, and
161 “burning” model predictions onto a raster. They also used vector operations to define and mask
162 the focal region, project, subset, buffer, convert to raster format (rasterize), locate random points,
163 and extract raster values at these points. Each workflow was designed to match the other as
164 closely as possible—i.e., in nearly all cases, a call of one function in one workflow matched a
165 call of a function with the same functionality on the equivalent data object in the other package.
166 The exceptions to this involved removal of temporary files and saving of specific rasters so they
167 did not get erased during temporary file deletion. These additional operations, plus any other
168 operations that did not use *terra* or *fasterRaster* functions were excluded in the final comparison
169 of workflow runtimes.

170 I implemented the same workflow on three regions of nested extents—a large region,
171 encompassing the entire area covered by the five river basins, a medium region focused on just
172 the Salween basin, and a small region on the Nam Loi subbasin of the Salween (Fig. S1). The
173 specific regions were chosen so that the same set of functions could be applied across each (e.g.,
174 converting country border vectors and vectors representing protected areas to raster format, etc.).

175 Since the workflow involved 50 sets of functions repeated for each of the cross-validation folds,
176 I report overall timing for 1) the “entire” workflow (including all 50 cross-validation folds), and
177 2) the “fold-averaged” workflow after averaging runtimes of functions used repeatedly across the
178 folds.

179 Of note, the *terra* `distance()` function used as-is was extremely slow and so would have
180 severely biased the comparison of runtimes. In preliminary runs of the medium-sized region, the
181 function could take weeks to run, much longer than all of the other functions’ runtimes
182 combined. (Newer versions of *terra* released since these tests were run allow users options that
183 can speed its operation, so may run faster than reported here). In the workflows, `distance()`
184 was used to calculate distance between forested cell centers and rivers and roads, which are
185 indicative of access to forest and so a risk factor (Soares-Filho et al., 2006). Since the purpose of
186 the analyses was intended to be illustrative, not indicative, of runtimes, I used an aggregation
187 “hack” to make comparisons fairer. For distance-based operations, I first reduced the number of
188 cells (made cells larger) using the `aggregate()` function, called `distance()` on the coarse-
189 resolution raster and respective vector, and then used `disaggregate()` to return the output to
190 the original resolution. Reducing the number of cells to which distances needed to be calculated
191 greatly sped *terra*’s `distance()` operation. However, aggregation also induced spatial
192 distortion in the predictors based on distance to roads and rivers (Fig. S2). This “hack” was used
193 only for the `distance()` operations.

194 Code for the benchmarking exercise is archived at
195 https://github.com/adamlilith/fasterRaster_benchmarking. For these exercises, I used *terra*
196 version 1.8-54 and *fasterRaster* version 8.4.1.0 connected to *GRASS* 8.4. All tests were run on a
197 Windows 11 Enterprise desktop computer with a Intel Xeon® 2592 MHz processor with 20-
198 cores and 40 logical processors, 512 GB RAM, and a 4-TB SSD. However, the workflows
199 limited both packages to using 4 cores and 64 GB of RAM, so neither package was allowed to
200 harness the full capacity of the system.

201 Results

202 The three study regions differed in size by orders of magnitude, with the largest containing >1.26
203 billion non-NA cells (Table 1). Based on the results from the large study region (run with the
204 *fasterRaster*-based workflow and no aggregation “hack” before application of the `distance()`
205 function), the risk of forest loss in 2000 was greatest in Cambodia (Fig. S1). Hereafter, I focus on
206 the relative runtimes of a *terra*- versus *fasterRaster*-based workflows.

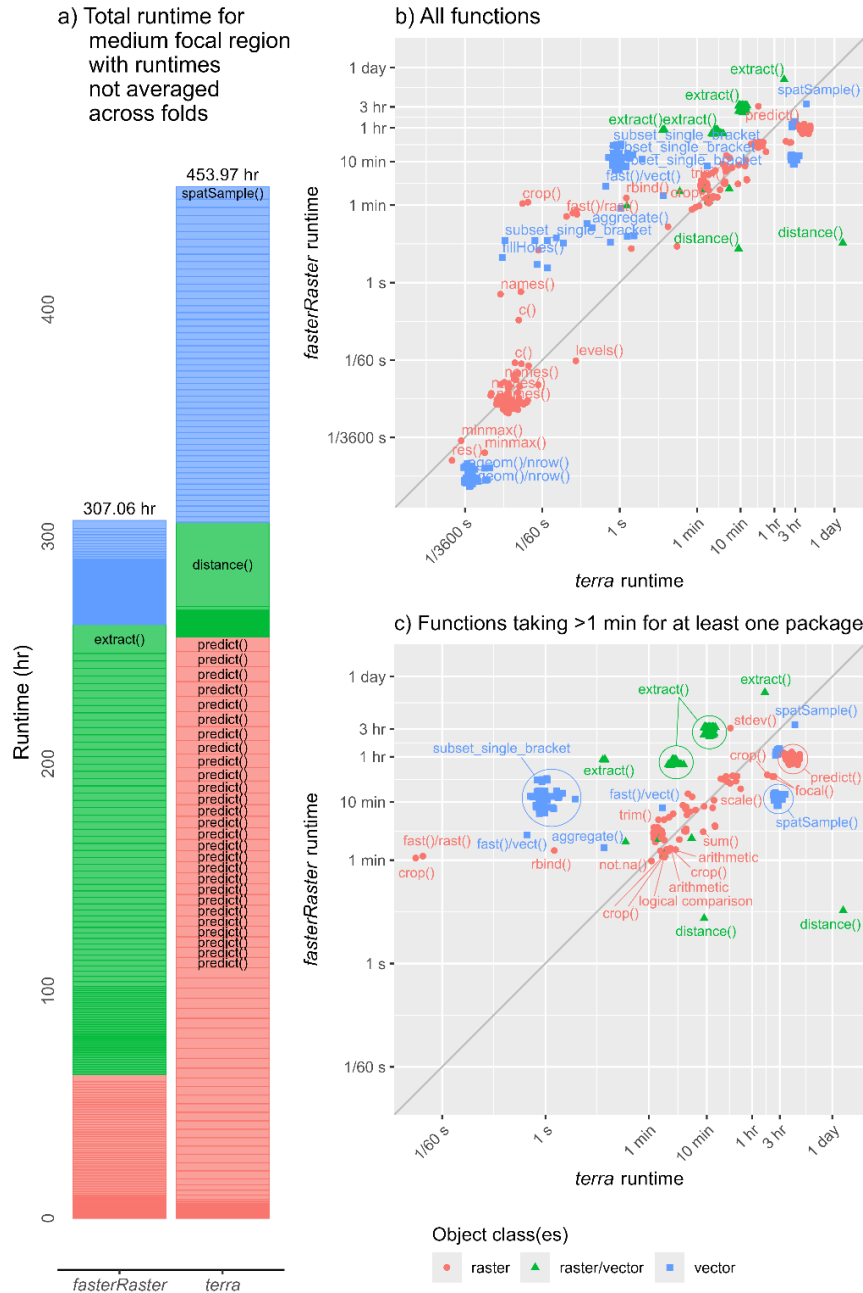
Table 1. Number of
30×30-m cells in each
study region.

Region	Non-NA cells
Small	17,189,027
Medium	180,001,073
Large	1,266,543,912

207

208 The large study region encompassing all five river basins was not workable for *terra*. The *terra*
209 `focal()` function worked for a 3-cell window but failed when the window was increased to 33
210 cells, causing *R* to crash. Multiple attempts were made. The `focal()` operation was
211 implemented before the `distance()` function was required, so for the *terra* workflow, the
212 aggregation “hack” was superfluous. In contrast, *fasterRaster* was able to complete the workflow
213 for the large region and did not need the cell aggregation “hack” to apply the `distance()`
214 function. The “entire” *fasterRaster* workflow runtime (with no cell aggregation) took ~27.5
215 weeks (4629 hr 52 min). Split across multiple *R* instances on the same computer, this required
216 about one month of wall time. These are sizable runtimes, but attest to *GRASS*’s ability to
217 manage very large-in-memory/large-on-disk spatial objects.

218 For the medium extent, the “entire” *fasterRaster* workflow was about 30% faster than the *terra*
219 workflow (Fig. 1). *fasterRaster* took less than 13 days (307 hr 4 min), whereas *terra* required
220 almost 19 days (453 hr 58 min). The `distance()` function was the slowest in the *terra*
221 workflow even after applying the aggregation “hack” in which larger cells were created from
222 composites of 512×512 cells. The `extract()` function took the most time in the *fasterRaster*
223 workflow. The “fold-averaged” *fasterRaster* runtime was twice as fast as the *terra* runtime (Fig.
224 2).



225

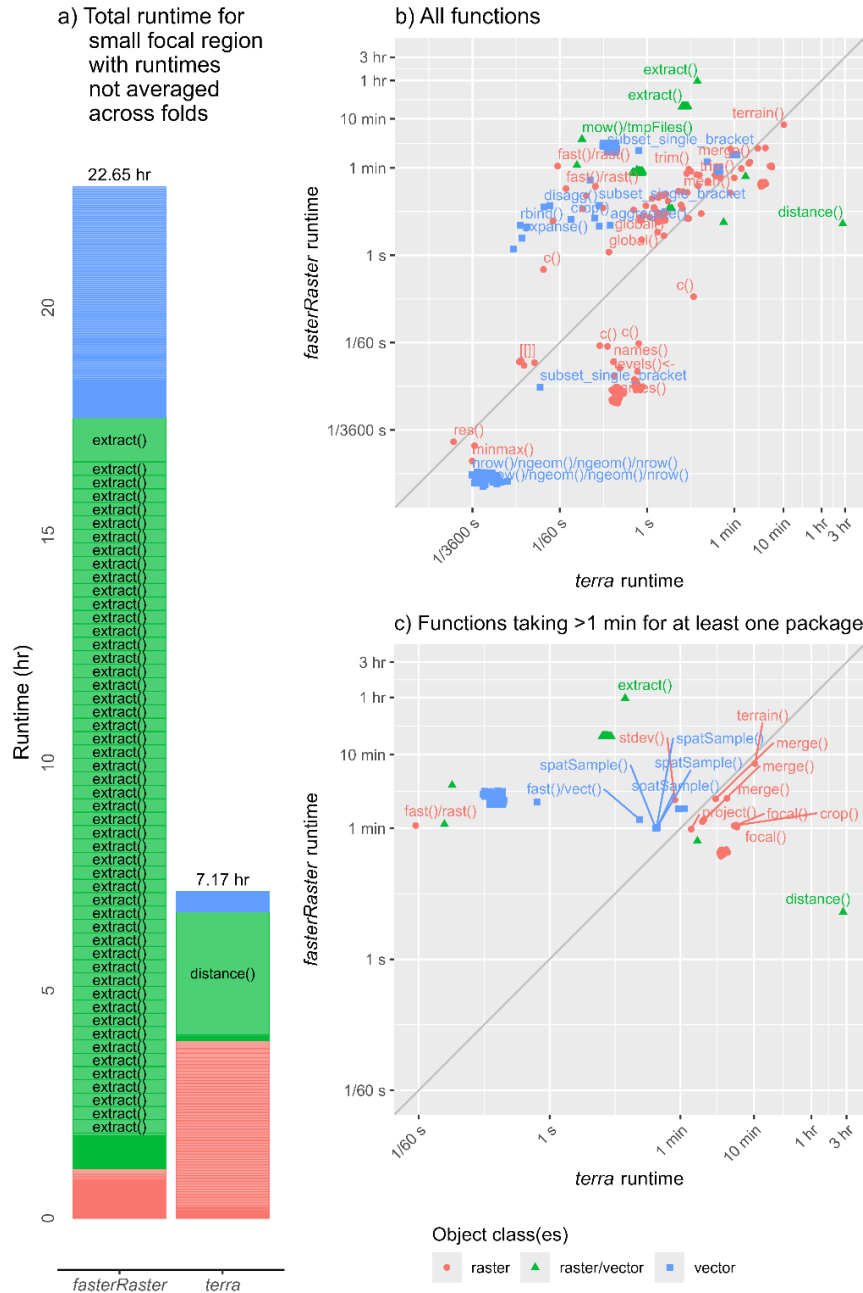
226 **Figure 1.** Comparison of runtimes for the “entire” workflow for the medium study region extent.
 227 In each panel, colors represent whether functions were run on rasters (red), vectors (green), or
 228 both (blue). (a) Comparison of total runtime. Bars are divided into smaller rectangles, one per
 229 function, and sorted within a class from fastest to slowest. Functions that took ≥ 15 min to
 230 execute are labeled. The `extract()` function was repeated across 50 folds and took the longest
 231 time in the *fasterRaster* workflow. Total runtime is shown at the top of each bar. (b) Comparison
 232 of runtime of the same functions in the *terra* and *fasterRaster* packages. (c) Runtime of functions
 233 that took at least 1 min to run in at least one workflow. For this analysis, cells were aggregated
 234 by a factor of 512 to speed the call of *terra*’s `distance()` function.



235

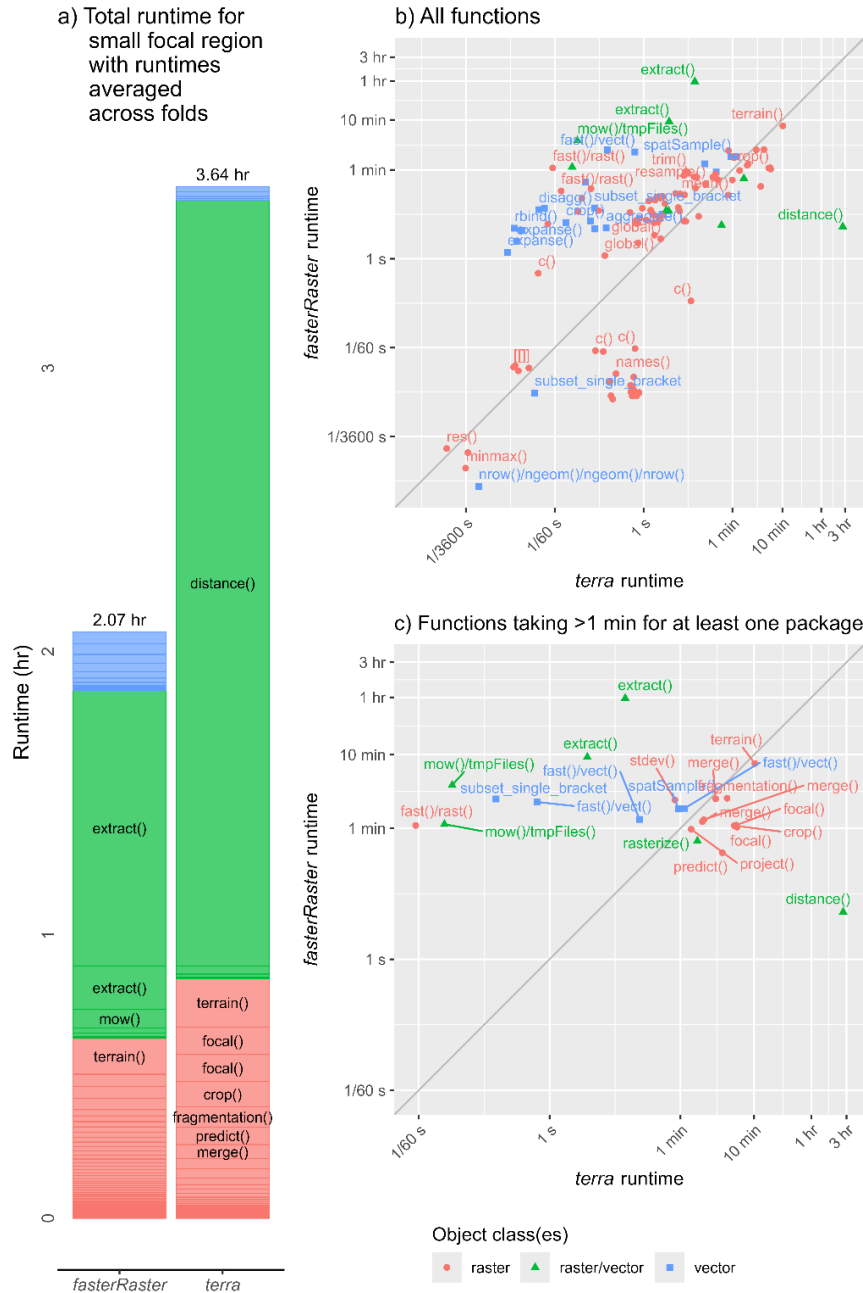
236 **Figure 2.** Comparison of “fold-averaged” runtimes for the medium study region extent. In each
 237 panel, colors represent whether functions were run on rasters (red), vectors (green), or both
 238 (blue). (a) Comparison of total runtime. Bars are divided into smaller rectangles, one per
 239 function, and sorted from slowest to fastest. Functions that took ≥ 15 min to execute are labeled.
 240 Total runtime is shown at the top of each bar. (b) Comparison of runtime of the same functions
 241 in the *terra* and *fasterRaster* packages. (c) Runtime of functions that took at least 1 min to run in
 242 at least one workflow. Cells were aggregated by a factor of 512 to speed the call of *terra*’s
 243 *distance()* function.

244 For workflows analyzing the small extent, the “entire” *fasterRaster* workflow was more than
245 three times slower than the *terra* workflow (Fig. 3). The *fasterRaster* workflow took nearly a day
246 (22 hr 39 min) to complete, whereas the *terra* workflow took less than a third of a day (7 hr 10
247 min). The `extract()` function was slowest in the *fasterRaster* workflow, and `distance()`
248 the slowest in the *terra* workflow. Since `extract()` was called once per fold, averaging
249 runtimes across crossvalidation folds calls greatly reduced the total runtime required by
250 *fasterRaster*’s `extract()`. As a result, the “fold-averaged” *fasterRaster* workflow was 1.76
251 times faster than the “fold-averaged” *terra* workflow (Fig. 4). These results are for cases where
252 the `distance()` function “hack” used an aggregation factor of 128. Aggregating cells by a
253 factor of 32 caused the “entire” and the “fold-averaged” *fasterRaster* runtimes to be much shorter
254 than the *terra* runtimes, while aggregating by 512 led to a 2- to 6-fold lead of *terra* over
255 *fasterRaster* (Figs. S3, S4, S5, and S6).



256

257 **Figure 3.** Comparison of runtimes for the “entire” workflow for the small study region. In each
 258 panel, colors represent whether functions were run on rasters (red), vectors (green), or both
 259 (blue). (a) Comparison of total runtime. Bars are divided into smaller rectangles, one per
 260 function, and sorted from slowest to fastest. Functions that took ≥ 15 min to execute are labeled.
 261 The `extract()` function was repeated across 50 crossvalidation folds and took the longest time
 262 the `fasterRaster` workflow. Total runtime is shown at the top of each bar. (b) Comparison of
 263 runtimes of the same function from each package. (c) Runtime of functions that took at least 1
 264 min to run in at least one workflow. Cells were aggregated by a factor of 128 to speed the call of
 265 `terra`’s `distance()` function.



266

267 **Figure 4.** Comparison of runtimes for the “fold-averaged” workflow for the small study region.
 268 Runtimes of functions called across folds are averaged. In each panel, colors represent whether
 269 functions were run on rasters (red), vectors (green), or both (blue). (a) Comparison of total
 270 runtime. Bars are divided into smaller rectangles, one per function, and sorted from slowest to
 271 fastest. Functions that took ≥ 15 min to execute are labeled. Total runtime is shown at the top of
 272 each bar. (b) Comparison of runtime of the same functions from the two packages. (c) Runtime
 273 of functions that took at least 1 min to run in at least one workflow. Cells were aggregated by a
 274 factor of 128 to speed the call of *terra*’s `distance()` function.

275 **Conclusions**

276 The *fasterRaster* package brings the power of *GRASS* to *R* while facilitating interoperability with
277 *terra* and other geospatial *R* packages. The exercise demonstrated that in cases when spatial
278 objects are large (many cells or fine spatial detail), *GRASS*-based analysis through *fasterRaster*
279 can achieve significant performance gains.

280 Aside from *terra*, *sf*, and *stars*, *fasterRaster* shares the remit of several other *R*
281 packages (reviewed on CRAN Task View: Analysis of Spatial Data; [https://cran.R-](https://cran.R-project.org/web/views/Spatial.html)
282 [project.org/web/views/Spatial.html](https://cran.R-project.org/web/views/Spatial.html)), but is nonetheless unique in its capabilities. *fasterRaster*
283 relies heavily on *rgrass*, but *rgrass* can be used as-is to call *GRASS* tools. Package *qgisprocess*
284 connects to QGIS to conduct GIS operations, and like *fasterRaster*, provides a fully-featured GIS
285 platform (Baghdadi et al., 2018). However, like *rgrass*, users need to understand the special
286 syntax of each tool to call it, and this can vary quite widely from syntax familiar to users of *R*.
287 Package *gdalraster* has special capacity to manage large raster and vector datasets, but also
288 requires more technical knowledge to run usefully (Toney, 2023).

289 Despite its strengths, *fasterRaster* does differ from *terra* in ways users should be aware. First,
290 many methods may have the same name and general functionality, but will not necessarily
291 produce the exact same outputs. For example, *terra*'s `distance()` function by default
292 calculates the distance from the center of a raster cell to the closest part of a lines vector
293 (Hijmans, 2025). In contrast, the *fasterRaster* `distance()` function uses *GRASS*'s
294 `r.grow.distance` tool, which first rasterizes the vector so each cell is demarked as “occupied”
295 or “unoccupied” by a line segment, then calculates the distance between a focal cell’s center and
296 the center of the nearest occupied cell. As a result, *fasterRaster*'s `distance()` output can differ
297 from *terra*'s by up to the linear dimensions of a cell. (Newer versions of *terra*'s `distance()`
298 have an option to use this same procedure). Differences have also been observed in
299 `resample()`, `project()`, and other functions, though discrepancies can be data-specific. As a
300 result, users should not expect *fasterRaster* functions to be exact replacements of those in *terra*.
301 Second, *fasterRaster* relies on temporary files (as does *terra*), but these have less protection from
302 automated disk-cleaning tools found on some operating systems like MS Windows 11’s “Storage
303 Sense.” If left running, these tools can delete temporary files and “break” GRasters and
304 GVectors. Relatedly, the disadvantage of a disk-heavy processing system like *GRASS* is that
305 while it may reduce memory requirements, it can fill the disk with lots of unused temporary files.
306 To address this, *fasterRaster* contains automated routines to remove most of these temporary
307 files. However, users can also manually call the `mow()` function to remove extraneous files,
308 though it must be done carefully to avoid breaking existing G-objects.

309 Future development will focus on expanded functionality and ease of use. *GRASS* has a wealth of
310 additional tools that do not yet appear in *fasterRaster*. These include tools for remote sensing,
311 hydrology, time series, and LiDAR data, among others. Moreover, the *GRASS* software has been
312 under constant development since its inception 1982, with new tools and functionality added

313 each sub-minor version (*GRASS* history website, no date). All of these represent opportunities
314 for further development. *fasterRaster* syntax mirrors that of *terra*, but depending on demand,
315 future development may also create *sf*-analogous functions so users familiar with that package
316 can more easily switch between it and *fasterRaster*.

317 The *fasterRaster* package is versioned in a manner to assist users in tracking which version of
318 *GRASS* interfaces with the package. Namely, *fasterRaster* versions will look something like
319 8.4.1.2, or more generally, *M1.M2.S1.S2*. Here, *M1.M2* mirror the version of *GRASS* for which
320 *fasterRaster* was built and tested. For example, *fasterRaster* version 8.4.x.x will work using
321 *GRASS* 8.4 (and backwards with version 8.3). The values in *S1.S2* refer to "major" and "minor"
322 versions of *fasterRaster*. That is, a change in the value of *S1* (e.g., from x.x.1.0 to x.x.2.0)
323 indicates changes that potentially break older code developed with a prior version of
324 *fasterRaster*. A change in *S2* refers to a bug fix, additional functionality in an existing function,
325 or the addition of an entirely new function. The *M1.M2* and *S1.S2* values increment
326 independently. For example, if the version changes from 8.4.1.5 to 8.5.1.5, then the new version
327 has been tested on *GRASS* 8.5, but code developed with version 8.4.1.x of *fasterRaster* should
328 still work.

329 Contributions, issues, and feature requests can be reported on the *fasterRaster* GitHub repository
330 at <https://github.com/adamlilith/fasterRaster>.

331 **Literature cited**

332 Baghdadi, N., Mallet, C., & Zribi, M. (Eds.). (2018). *QGIS and Generic Tools*. Wiley. doi:
333 10.1002/9781119457091

334 Bivand, R. P. S. (2025). *rgrass*: Interface between ‘GRASS’ Geographical Information System
335 and ‘R’ (R package version 0.5-3) [Computer software].
336 <https://doi.org/10.32614/CRAN.package.rgrass>

337 Booth, T. H., Nix, H. A., Busby, J. R., & Hutchinson, M. F. (2014). BIOCLIM: The first species
338 distribution modeling package, its early applications and relevance to most current MaxEnt
339 studies. *Diversity and Distributions*, 20, 1–9. doi: 10.1111/ddi.12144

340 Gao, B.-C. (1996). NDWI — A normalized difference water index for remote sensing of
341 vegetation liquid water from space. *Remote Sensing of Environment*, 58, 257–266. doi:
342 10.1016/S0034-4257(96)00067-3

343 *GRASS* Development Team. (2025a). *Geographic Resources Analysis Support System (GRASS)*
344 software (Version 8.4) [Computer software]. Open Source Geospatial Foundation.
345 <https://grass.osgeo.org>

346 *GRASS* Development Team. (2025b). *Geographic Resources Analysis Support System (GRASS)*
347 programmer’s manual [Computer software]. Open Source Geospatial Foundation.
348 <https://grass.osgeo.org/programming8>

349 Hansen, M. C., Potapov, P. V., Moore, R., Hancher, M., Turubanova, S. A., Tyukavina, A.,
350 Thau, D., Stehman, S. V., Goetz, S. J., Loveland, T. R., Kommareddy, A., Egorov, A., Chini, L.,
351 Justice, C. O., & Townshend, J. R. G. (2013). High-resolution global maps of 21st-century forest
352 cover change. *Science*, *342*, 850–853. doi: 10.1126/science.1244693

353 Hijmans, R. (2025). *terra: Spatial data analysis* (R package version 1.8-60) [Computer
354 software]. <https://doi.org/10.32614/CRAN.package.terra>

355 Hughes, A.C. (2017). Understanding the drivers of Southeast Asian biodiversity loss. *Ecosphere*,
356 *8*, e01624. doi: 10.1002/ecs2.1624

357 Jasiewicz, J., & Stepinski, T. (2013). Geomorphons – A pattern recognition approach to
358 classification and mapping of landforms. *Geomorphology*, *182*, 147–156. doi:
359 10.1016/j.geomorph.2012.11.005

360 Neteler, M., Bowman, M. H., Landa, M., & Metz, M. (2012). *GRASS GIS: A multi-purpose open*
361 *source GIS. Environmental Modelling & Software*, *31*, 124–130. doi:
362 10.1016/j.envsoft.2011.11.014

363 Pebesma, E., & Bivand, R. P. S. (2023). *Spatial Data Science: With Applications in R*. Chapman
364 and Hall/CRC. doi: <https://doi.org/10.1201/9780429459016>

365 Pebesma, E. (2018). Simple features for R: Standardized support for spatial vector data. *The R*
366 *Journal*, *10*, 439–446. doi: 10.32614/RJ-2018-009

367 Qi, J., Chehbouni, A., Huete, A. R., Kerr, Y. H., & Sorooshian, S. (1994). A modified soil
368 adjusted vegetation index. *Remote Sensing of Environment*, *48*, 119–126. doi: 10.1016/0034-
369 4257(94)90134-1

370 Riitters, K., J. Wickham, R. O'Neill, B. Jones, & E. Smith. (2000). Global-scale patterns of forest
371 fragmentation. *Conservation Ecology*, *4*:3. URL: <http://www.consecol.org/vol4/iss2/art3/>. Errata:
372 <https://www.ecologyandsociety.org/vol4/iss2/art3/errata/january26.2001.html>.

373 Soares-Filho, B.S., Nepstad, D.C., Curran, L.M., Cerqueira, G.C., Garcia, R.A., Ramos, C.A.,
374 Voll, E., McDonald, A., Lefebvre, P., & Schlesinger, P. (2006). Modelling conservation in the
375 Amazon basin. *Nature*, *440*, 520-523. doi: 10.1038/nature04389

376 Stepinski, T., & Jasiewicz, J. (2011). Geomorphons – A new approach to classification of
377 landforms. In T. Hengl, I. S. Evans, J. P. Wilson, & M. Gould (Eds.), *Proceedings of*
378 *Geomorphometry* (pp. 109–112). Redlands. doi: 10.1016/j.geomorph.2012.11.005

379 Toney, C. (2025). *gdalraster: R bindings to the “Geospatial Data Abstraction Library” raster*
380 *API* [Computer software]. USDA Forest Service, Rocky Mountain Research Station.
381 <https://usdaforestservice.github.io/gdalraster/>

382 Wang, Y., Hollingsworth, P.M., Zhai, D., West, C.D., Green, J.M.H., Chen, H., Hurni, K., Su,
383 Y., Warren-Thomas, E., Xu, J., & Ahrends, A. (2023). High-resolution maps show that rubber
384 causes substantial deforestation. *Nature*, 623, 340-346. doi: 10.1038/s41586-023-06642-z

385 Wickham, H., Hesselberth, J., Salmon, M., Roy, O., & Brüggenmann, S. (2025). *pkgdown: Make*
386 *static HTML documentation for a package* (R package version 2.1.3) [Computer software].
387 <https://pkgdown.r-lib.org/>

1 **Supplement to: *fasterRaster*: GIS in R using GRASS for large vectors and rasters**

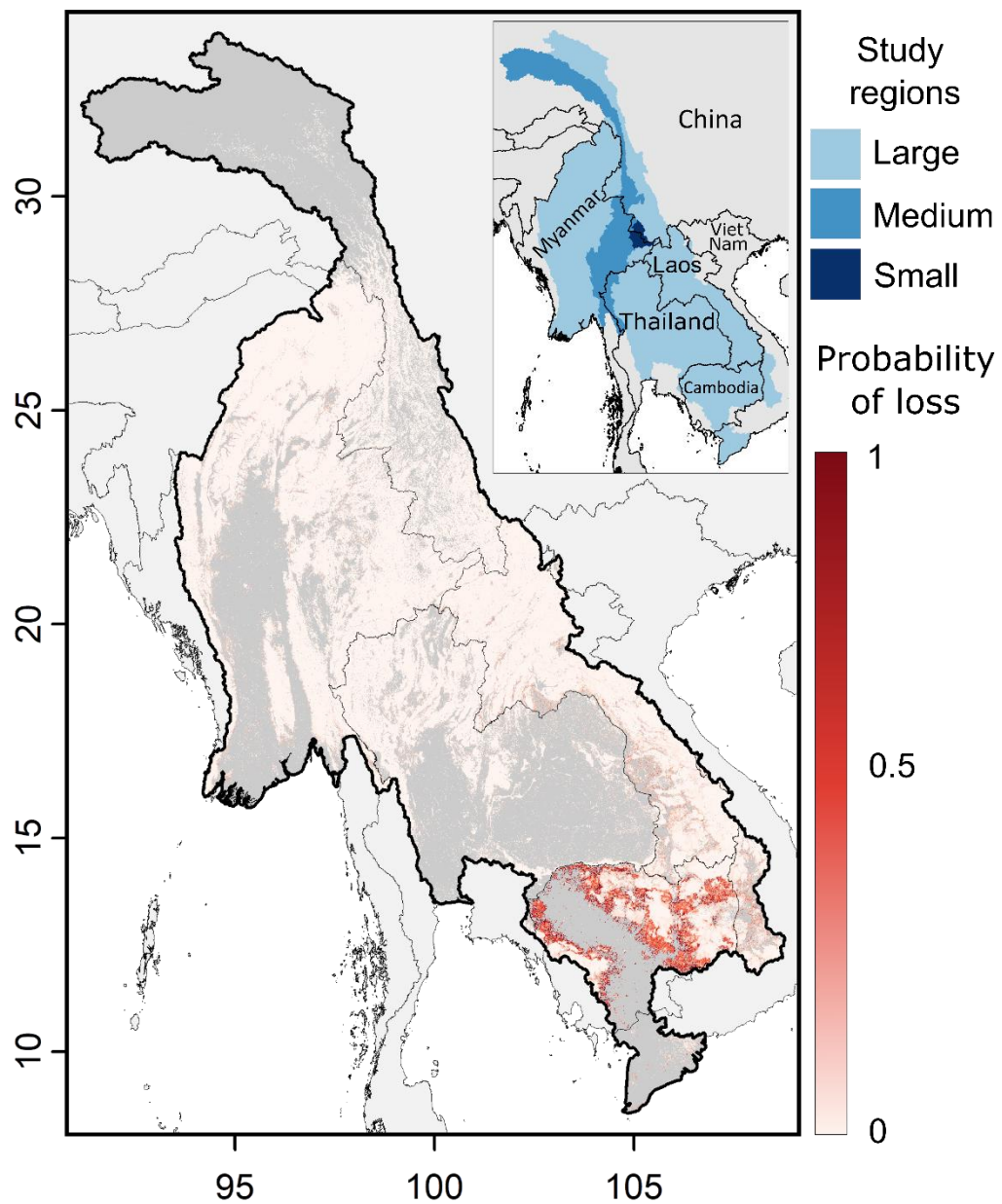
2 **Author:** Adam B. Smith

3 **Published in:** *Transactions in GIS*, doi: [10.1111/tgis.70238](https://doi.org/10.1111/tgis.70238)

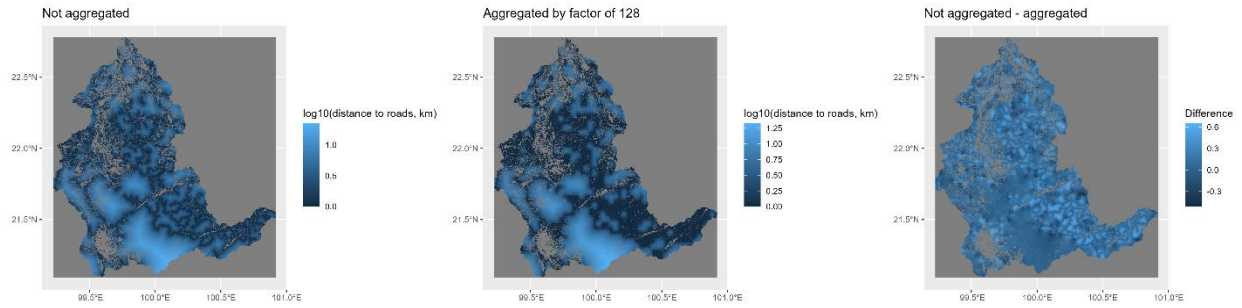
Table S1. Source and characteristics of predictors and response variable included in the workflows used to assess performance of *fasterRaster*.

Input	Derived from	Original			Source
		Resolution	CRS	Values	
Watershed basin polygons	Watershed basins polygons (vector)	—	WGS84	—	FAO, 2022a
Forest loss/persistence (response variable)	Forest cover for 2000 and 2020 (raster)	$0.00025^\circ \times 0.00025^\circ$	WGS84	Integer (0/1)	Potapov et al., 2021
Forest density, 33×33-cell neighborhood (P)	Forest cover in 2000 (raster)	$0.00025^\circ \times 0.00025^\circ$	WGS84	Integer (0-1089)	Potapov et al., 2021
Forest fragmentation class in 3×3-cell neighborhood (P)	Forest cover in 2000 (raster)	$0.00025^\circ \times 0.00025^\circ$	WGS84	Factor	Potapov et al., 2021 & Riitters et al., 2000
Elevation (P)	Elevation (raster)	$0.0003282^\circ \times 0.0003282^\circ$	WGS84	Continuous	MapZen (n.d.)
Slope, fine-scale (P)	Elevation, fine-scale (raster)	$0.0003282^\circ \times 0.0003282^\circ$	WGS84	Continuous	MapZen (n.d.)
Slope, coarse-scale (P)	Elevation, coarse-scale (raster)	$0.0052579^\circ \times 0.0052579^\circ$		Continuous	MapZen (n.d.)
Short vegetation in 33×33-cell neighborhood (P)	Land use/land cover (raster)	$0.00025^\circ \times 0.00025^\circ$	WGS84	Integer (0-1089)	Potapov et al., 2022
Human population density in 33×33-cell neighborhood (P)	Population density in 2000 (raster)	100×100 m	Mollweide	Continuous	European Commission, 2023

Distance to nearest major river (P)	Rivers (vector)	(Calculated from response raster)	WGS84	Continuous	FAO 2022b
Distance to nearest major road (P)	Roads (vector)	(Calculated from response raster)	WGS84	Continuous	OSM, 2024
Protected area (P)	Protected areas (vector)	(Calculated from response raster)	WGS84	Binary factor	UNEP-WCMC & IUCN, 2024
Country (P)	Countries (vector)	(Calculated from response raster)	WGS84	Factor	GADM, 2022
Protected area × country	From protected areas and countries (vectors)	(Calculated from response raster)	WGS84	Factor	UNEP-WCMC & IUCN, 2024; GADM, 2022

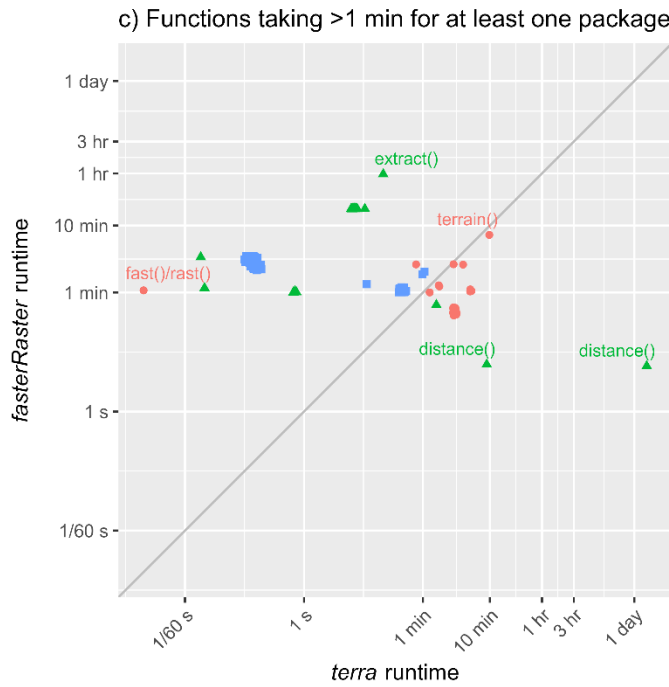
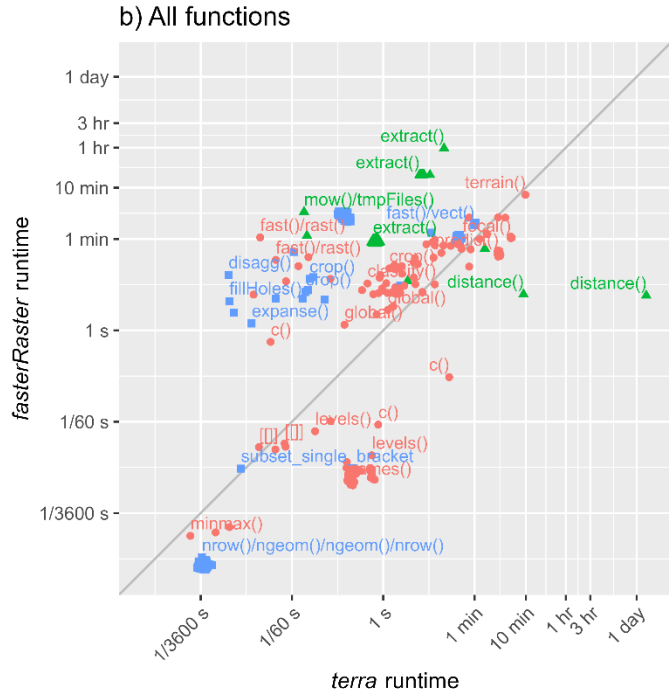
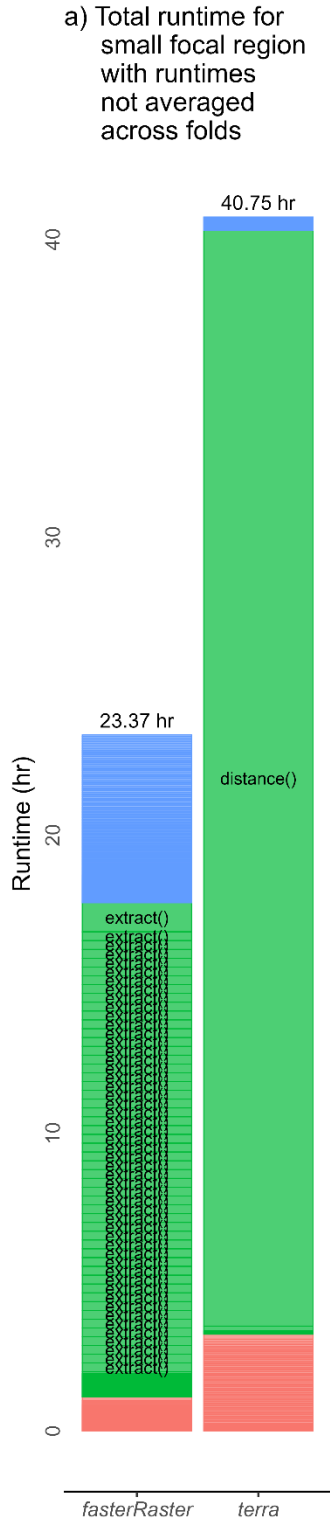


5
 6 **Figure S1.** Study region and predicted probability of forest cover loss between 2000 and 2020
 7 based on analysis of the large study region. The map of forest loss probability was created using
 8 the *fasterRaster* workflow without the aggregation “hack” to accommodate the `distance()`
 9 function.



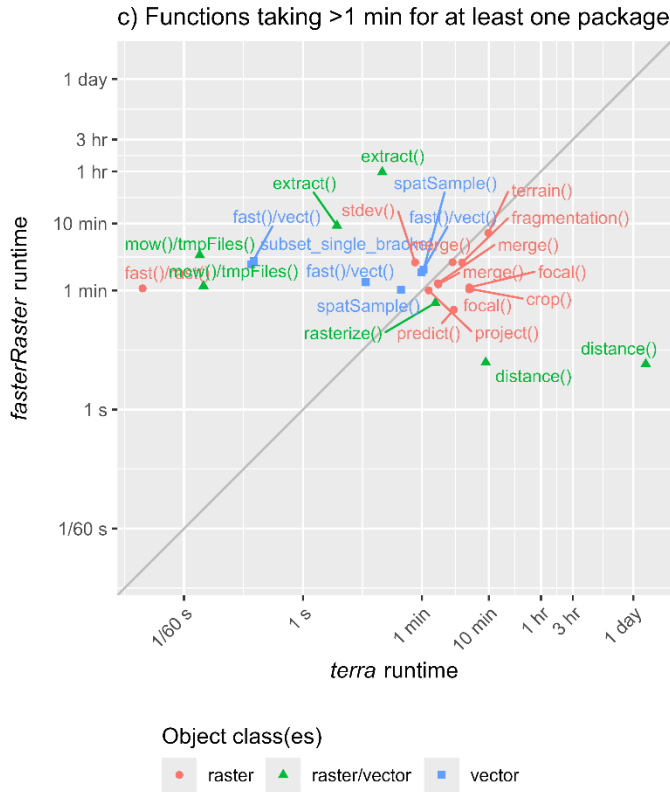
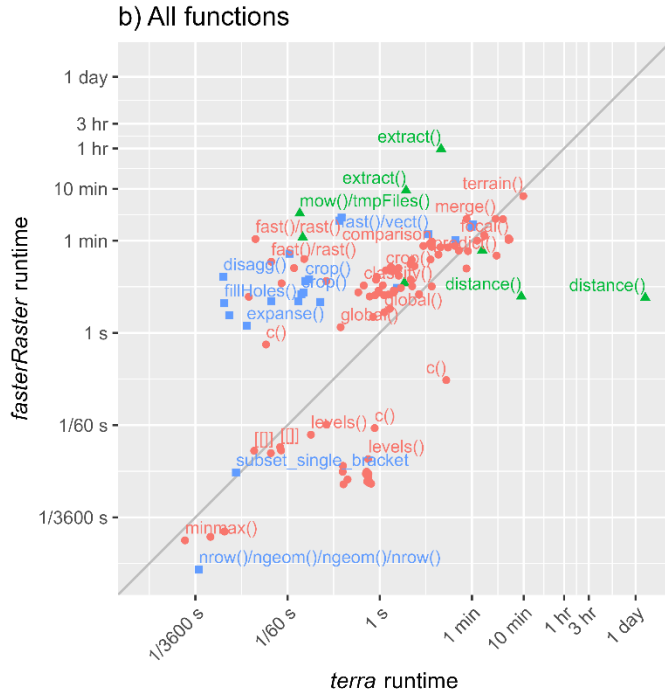
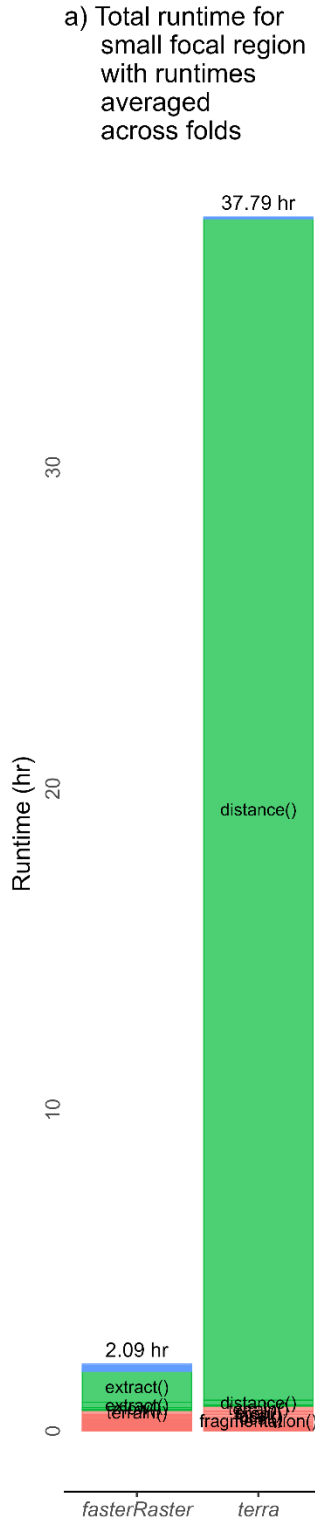
10

11 **Figure S2.** Effect of aggregating cells to speed the call of *terra*'s `distance()` function which
 12 would otherwise dominate the runtimes. Cell aggregation, then resampling, induces artifacts in
 13 the output. The small study region (subbasins of the Salween river basin) are shown for
 14 illustration. Here, cells were aggregated by a factor of 128, the effect of which is visible in the
 15 map on the right which displays the difference between the two maps to its left.



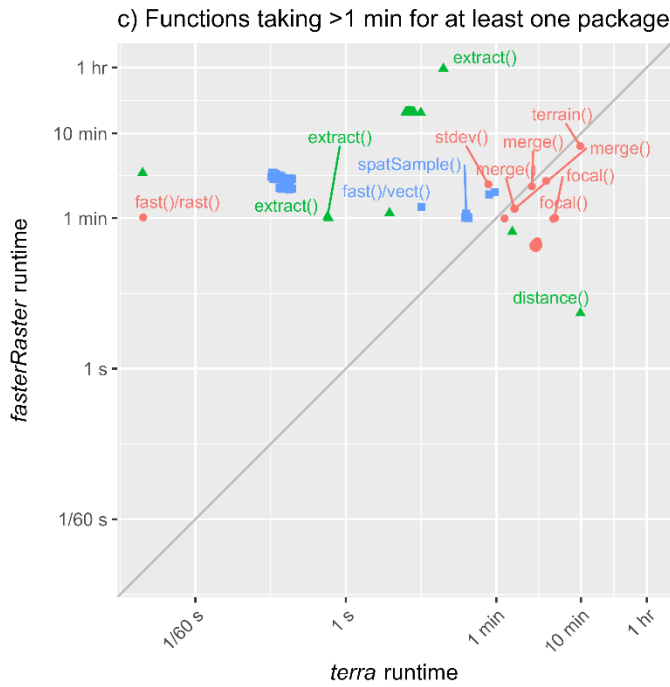
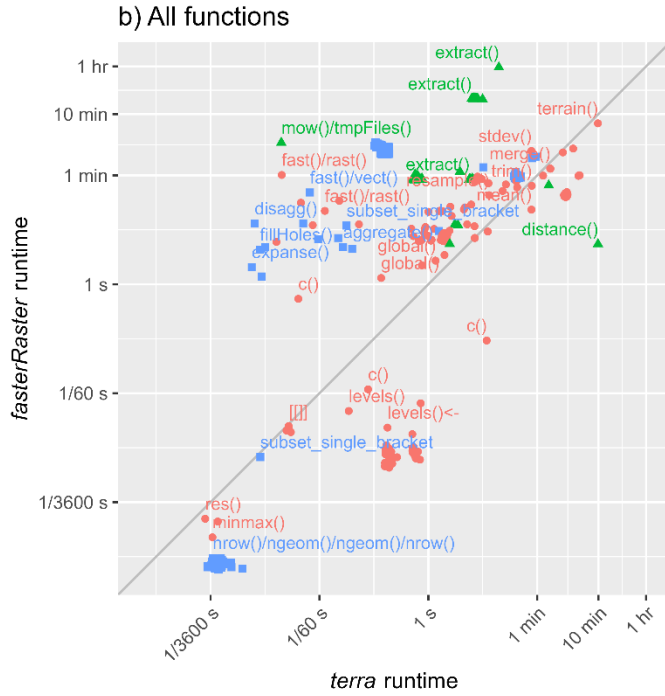
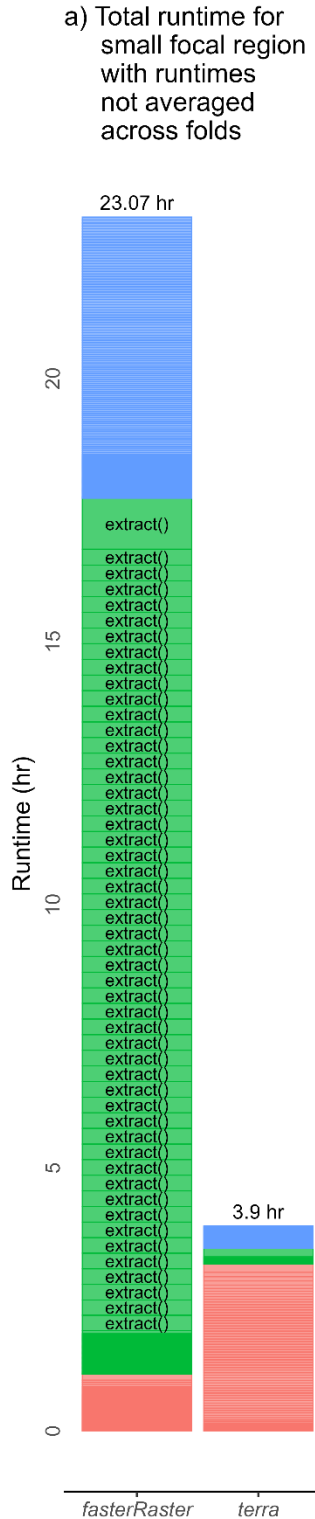
16

17 **Figure S3.** Comparison of runtimes “entire” workflow for the **small** study region extent when
 18 cells were aggregated by a factor of **32**.



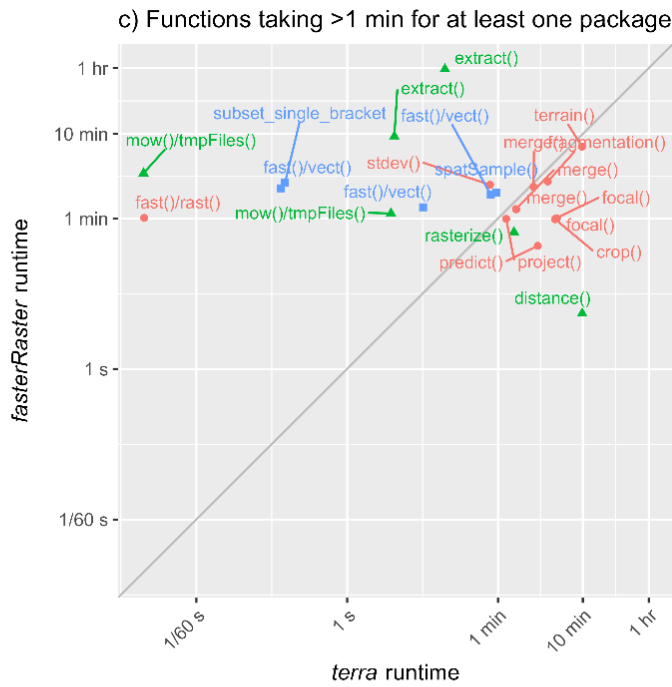
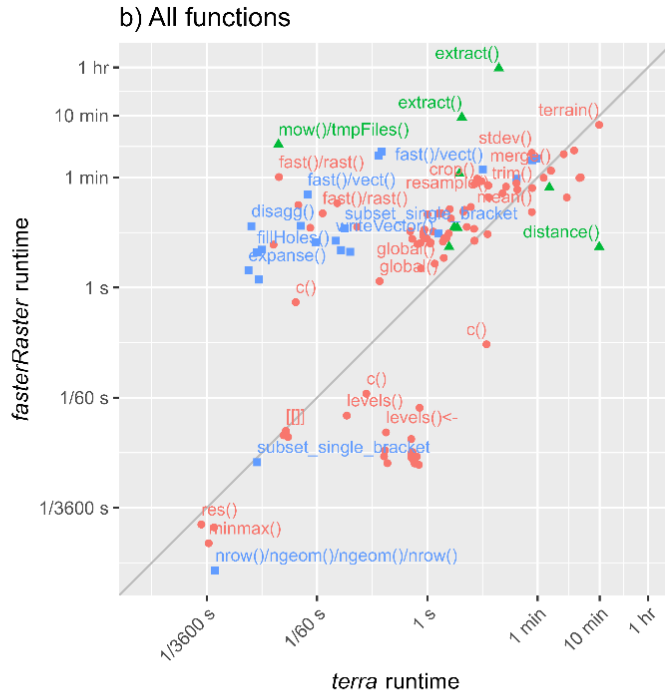
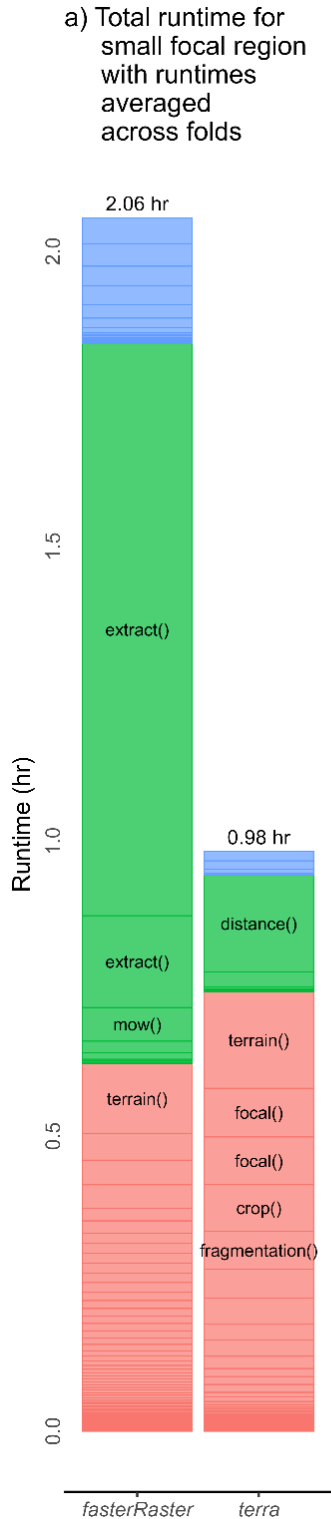
19

20 **Figure S4.** Comparison of runtimes “fold-averaged” workflow for the **small** study region extent
 21 when cells were aggregated by a factor of **32**.



22

23 **Figure S5.** Comparison of runtimes “entire” workflow for the **small** study region extent when
 24 cells were aggregated by a factor of **512**.



25

26 **Figure S6.** Comparison of runtimes “fold-averaged” workflow for the **small** study region extent
 27 when cells were aggregated by a factor of 512.

28 Supplemental Literature Cited

- 29 European Commission. (2024). *GHSL data package 2023* (JRC133256). Publications Office of
30 the European Union. <https://doi.org/10.2760/098587>
- 31 Food and Agriculture Organization of the United Nations. (2022a). *Hydrological basins in*
32 *Southeast Asia* [Data set]. FAO AQUASTAT.
33 <https://data.apps.fao.org/catalog/organization/fao-aquastat>
- 34 Food and Agriculture Organization of the United Nations. (2022b). *Rivers of South and East*
35 *Asia* [Data set]. FAO AQUASTAT. [https://data.apps.fao.org/catalog/organization/fao-](https://data.apps.fao.org/catalog/organization/fao-aquastat)
36 [aquastat](https://data.apps.fao.org/catalog/organization/fao-aquastat)
- 37 GADM. (2022). *Database of global administrative areas* (Version 4.1) [Data set].
38 <https://gadm.org>
- 39 Mapzen. (n.d.). *Terrain Tiles: A global dataset providing bare-earth terrain heights, tiled for*
40 *easy usage and provided on S3* [Data set]. Linux Foundation. Retrieved October 1, 2024,
41 from <https://registry.opendata.aws/terrain-tiles>
- 42 OpenStreetMap contributors. (2024). *OpenStreetMap data extracts* [Data set]. Geofabrik.
43 <https://download.geofabrik.de>
- 44 Potapov, P., Hansen, M. C., Pickens, A., Hernandez-Serna, A., Tyukavina, A., Turubanova, S.,
45 Zalles, V., Li, X., Khan, A., Stolle, F., & Harris, N. (2022). The global 2000–2020 land cover
46 and land use change dataset derived from the Landsat archive: First results. *Frontiers in*
47 *Remote Sensing*, 3, 856903. <https://doi.org/10.3389/frsen.2022.856903>
- 48 Potapov, P., Li, X., Hernandez-Serna, A., Tyukavina, A., Hansen, M. C., Kommareddy, A.,
49 Pickens, A., Turubanova, S., Tang, H., Silva, C. E., Armston, J., Dubayah, R., Blair, J. B., &
50 Hofton, M. (2021). Mapping global forest canopy height through integration of GEDI and
51 Landsat data. *Remote Sensing of Environment*, 253, 112165.
52 <https://doi.org/10.1016/j.rse.2020.112165>
- 53 Riitters, K., Wickham, J., O'Neill, R., Jones, B., & Smith, E. (2000). Global-scale patterns of
54 forest fragmentation. *Conservation Ecology*, 4(2), 3. <http://www.consecol.org/vol4/iss2/art3/>
55 Errata: <https://www.ecologyandsociety.org/vol4/iss2/art3/errata/january26.2001.html>
- 56 UNEP-WCMC, & IUCN. (2024). *Protected Planet: The World Database on Protected Areas*
57 *(WDPA)* (Version 1.6, May 2024) [Data set]. UNEP-WCMC and IUCN.
58 <https://www.protectedplanet.net>